

# Mass and energy balance calculations for an artificial ice reservoir (Icestupa)

Suryanarayanan Balasubramanian<sup>1,\*</sup>, Martin Hoelzle<sup>1</sup>, Michael Lehning<sup>2</sup>,  
Sonam Wangchuk<sup>3</sup>, Johannes Oerlemans<sup>4</sup> and Felix Keller<sup>5</sup>

<sup>1</sup>University of Fribourg, Fribourg, Switzerland

<sup>2</sup>WSL Institute for Snow and Avalanche Research, Davos, Switzerland

<sup>3</sup>Himalayan Institute of Alternatives Ladakh, Leh, India

<sup>4</sup>Institute for Marine and Atmospheric Research, Utrecht University, Utrecht, The Netherlands

<sup>5</sup>Academia Engiadina, Samedan, Switzerland

Correspondence\*:

Suryanarayanan Balasubramanian

suryanarayanan.balasubramanian@unifr.ch

## 1 MODEL SETUP

- 2 A bulk energy and mass balance model is used to calculate the amounts of ice, meltwater, water vapour and
- 3 runoff water of the AIR every hour. This model consists of four modules which calculate its, a) geometric
- 4 evolution, b) energy balance c) surface temperature and d) mass balance as shown schematically in Fig. 1.

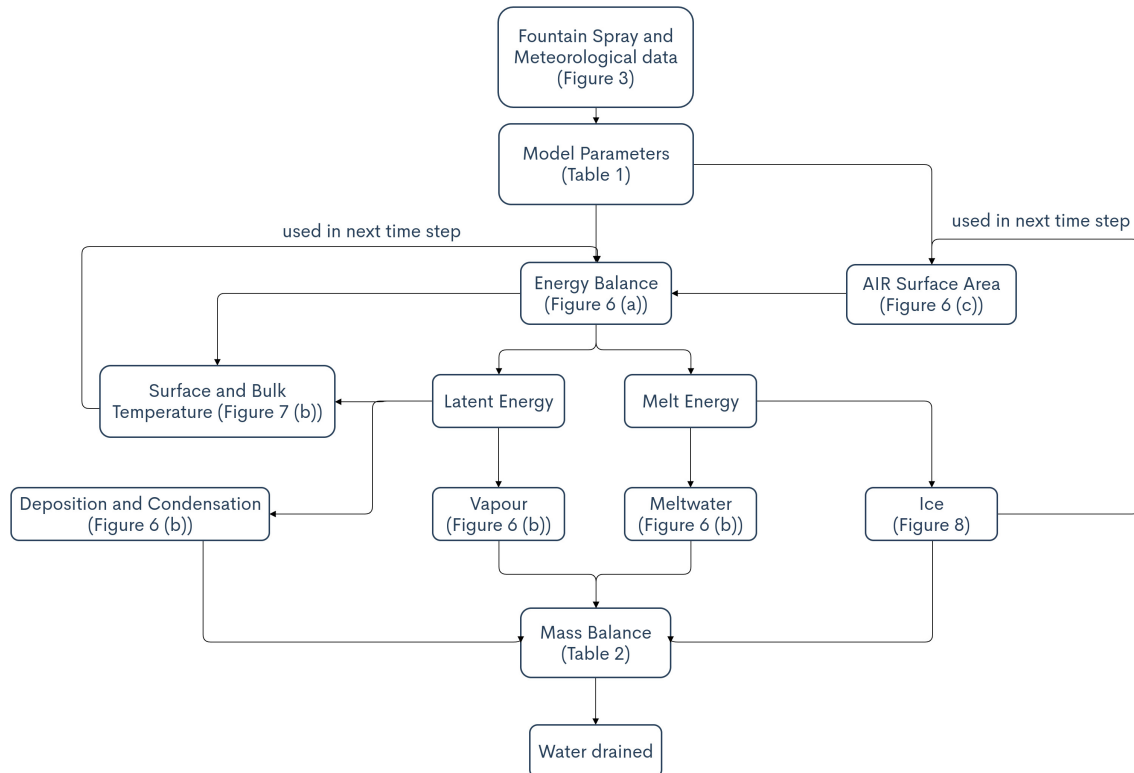


**Figure 1.** Model schematic showing the algorithm used in the model at every time step. Further details about the variables can be found in the associated tables and figures.

## 1.1 Geometric evolution

Radius  $r_{ice}^i$  and height  $h_{ice}^i$  define the dimensions of the Icestupa assuming its geometry to be a cone as shown in Fig. 2. The surface area  $A^i$  exposed to the atmosphere and volume  $V^i$  are:

$$A = \pi \cdot r_{ice} \cdot \sqrt{r_{ice}^2 + h_{ice}^2} \quad (1)$$

$$V = \pi/3 \cdot r_{ice}^2 \cdot h_{ice} \quad (2)$$

Note that we do not specify the time step superscript  $i$  of the shape variables  $A$ ,  $V$ ,  $r_{ice}$  and  $h_{ice}$  for brevity. The equations used henceforth display model time step superscript  $i$  only if it is different from the current time step.

With the mass of the Icestupa  $M_{ice}$ , its current volume can also be expressed as:

$$V = M_{ice}/\rho_{ice} \quad (3)$$

where  $\rho_{ice}$  is the density of ice ( $917 \text{ kg m}^{-3}$ ). The model of the Icestupa is initialised with a thickness of  $\Delta x$  (defined in 1.2) and a circular area of radius  $r_F$ . The constant  $r_F$  represents the mean spray radius of the fountain. This fountain spray radius is determined by

During subsequent time steps, the dimensions of the Icestupa evolve assuming a uniform ice formation and decay across its surface area with an invariant slope  $s_{cone} = \frac{h_{ice}}{r_{ice}}$  as shown in Fig. 2. During these time steps, the volume is parameterised using Eqn. 2 as:

$$V = \pi/3 \cdot r_{ice}^3 \cdot s_{cone} \quad (4)$$

However, the Icestupa cannot outgrow the maximum range of the water droplets ( $(r_{ice})_{max} = r_F$ ). Combining equations 2, 3 and 4, the geometric evolution of the Icestupa at each time step  $i$  can be determined by considering the following rules:

$$(r_{ice}, h_{ice}) = \begin{cases} (r_F, \Delta x) & \text{if } i = 0 \\ (r_{ice}^{i-1}, \frac{3 \cdot M_{ice}}{\pi \cdot \rho_{ice} \cdot (r_{ice}^{i-1})^2}) & \text{if } r_{ice}^{i-1} \geq r_F \text{ and } \Delta M_{ice} > 0 \text{ where } \Delta M_{ice} = M_{ice}^{i-1} - M_{ice}^{i-2} \\ (\frac{3 \cdot M_{ice}}{\pi \cdot \rho_{ice} \cdot s_{cone}})^{1/3} \cdot (1, s_{cone}) & \text{otherwise} \end{cases} \quad (5)$$

## 1.2 Energy Balance

The energy balance equation (Hock, 2005) for the Icestupa is formulated as follows:

$$q_{SW} + q_{LW} + q_L + q_S + q_F + q_G = q_{surf} \quad (6)$$

where  $q_{surf}$  is the surf energy flux in  $[W m^{-2}]$ ;  $q_{SW}$  is the surf shortwave radiation;  $q_{LW}$  is the surf longwave radiation;  $q_L$  and  $q_S$  are the turbulent latent and sensible heat fluxes.  $q_F$  represents the heat exchange of the fountain water droplets with the AIR ice surface.  $q_G$  represents ground heat flux between Icestupa surface and Icestupa interior. Energy transferred in the direction of the ice surface is always denoted as positive and away as negative.

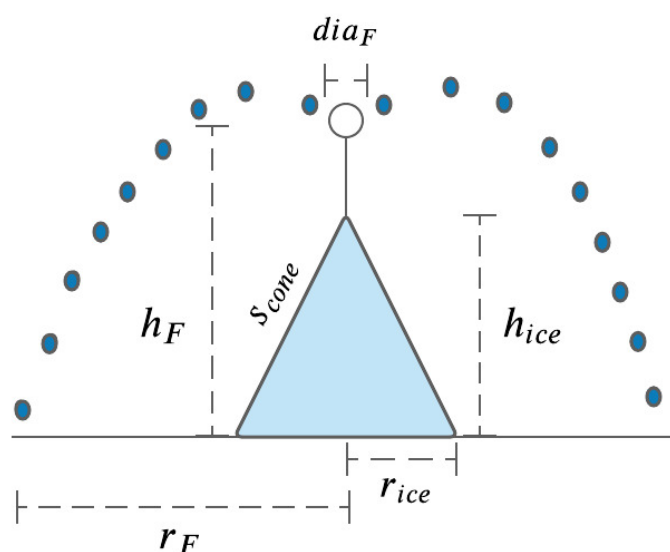


**Figure 2.** Shape variables and fountain constants of the EP Icestupa.  $r_{ice}$  is the radius,  $h_{ice}$  is the height and  $s_{cone}$  is the slope of the ice cone.  $r_F$  is the spray radius,  $h_F$  is the height and  $dia_F$  is the nozzle diameter of the fountain.

Equation 6 is usually referred to as the energy budget for “the surface”, but practically it must apply to a surface layer of ice with a finite thickness  $\Delta x$ . The energy flux acts upon the Icestupa surface layer which has an upper and a lower boundary defined by the atmosphere and the ice body of the Icestupa, respectively. The parameter selection for  $\Delta x$  is based on the following two arguments: (a) the ice thickness  $\Delta x$  should be small enough to represent the surface temperature variations every model time step  $\Delta t$  and (b)  $\Delta x$  should be large enough for these temperature variations to not reach the bottom of the surface layer. Therefore, we introduced a 20 mm thick surface layer for a model time step of 1 hour, over which the energy balance is calculated. A sensitivity analysis was later performed to understand the influence of this factor. Here, we define the surface temperature  $T_{ice}$  to be the modelled average temperature of the Icestupa surface layer and the energy flux  $q_{surf}$  is assumed to act uniformly across the Icestupa area  $A$ .

#### 1.2.1 Net Shortwave Radiation $q_{SW}$

The surf shortwave radiation  $q_{SW}$  is computed as follows:

$$q_{SW} = (1 - \alpha) \cdot (SW_{direct} \cdot f_{cone} + SW_{diffuse}) \quad (7)$$

where  $SW_{direct}$  and  $SW_{diffuse}$  are the ERA5 direct and diffuse short wave radiation,  $\alpha$  is the modelled albedo and  $f_{cone}$  is the area fraction of the ice structure exposed to the direct shortwave radiation.

We model the albedo using a scheme described in Oerlemans and Knap (1998). The scheme records the decay of albedo with time after fresh snow is deposited on the surface.  $\delta t$  records the number of time steps after the last snowfall event. After snowfall, albedo changes over a time step,  $\delta t$ , as

$$\alpha = \alpha_{ice} + (\alpha_{snow} - \alpha_{ice}) \cdot e^{(-\delta t)/\tau} \quad (8)$$

where  $\alpha_{ice}$  is the bare ice albedo value (0.35),  $\alpha_{snow}$  is the snow ice albedo value (0.85) and  $\tau$  is a decay rate, which determines how fast the albedo of the ageing snow reaches this value. The decay rate  $\tau$  is assumed to have a base value of 10 days similar to values obtained by Schmidt et al. (2017) for wet surfaces and its maximal value is set based on observations by Oerlemans and Knap (1998) as shown in Table 1. Furthermore, the albedo  $\alpha$  varies depending on the water source that formed the current Icestupa surface. Correspondingly, the albedo is reset to the value of bare ice albedo if the fountain is spraying water onto the current ice surface and to the value of fresh snow albedo if a snowfall event occurred. Snowfall events are assumed if the air temperature is below  $T_{ppt} = 1^\circ C$  (Fujita and Ageta, 2000).

The area fraction  $f_{cone}$  of the ice structure exposed to the direct shortwave radiation depends on the shape considered. The direct solar radiation incident on the AIR surface is first decomposed into horizontal and vertical components using the solar elevation angle  $\theta_{sun}$ . For a conical shape, half of the total curved surface is exposed to the vertical component of the direct shortwave radiation and the projected triangle of the curved surface is exposed to the horizontal component of the direct shortwave radiation. The solar elevation angle  $\theta_{sun}$  used is modelled using the parametrisation proposed by Woolf (1968). Accordingly,  $f_{cone}$  is determined as follows:

$$f_{cone} = \frac{(0.5 \cdot r_{ice} \cdot h_{ice}) \cdot \cos\theta_{sun} + (\pi \cdot r_{ice}^2 / 2) \cdot \sin\theta_{sun}}{\pi \cdot r_{ice} \cdot (r_{ice}^2 + h_{ice}^2)^{1/2}} \quad (9)$$

The ERA5 diffuse shortwave radiation is assumed to impact the conical Icestupa surface uniformly.

### 1.2.2 Net Longwave Radiation $q_{LW}$

The surf longwave radiation  $q_{LW}$ , for which there were no direct measurements available at EP, is determined as follows:

$$q_{LW} = LW_{in} - \sigma \cdot \epsilon_{ice} \cdot (T_{ice} + 273.15)^4 \quad (10)$$

where  $T_a$  represents the measured air temperature,  $T_{ice}$  is the modelled surface temperature, both temperatures are given in  $[^\circ C]$ ,  $\sigma = 5.67 \cdot 10^{-8} J m^{-2} s^{-1} K^{-4}$  is the Stefan-Boltzmann constant,  $LW_{in}$  denotes the incoming longwave radiation derived from the ERA5 dataset and  $\epsilon_{ice}$  is the corresponding emissivity value for the Icestupa surface (see Table 1).

### 1.2.3 Turbulent sensible $q_S$ and latent $q_L$ heat fluxes

The turbulent sensible  $q_S$  and latent heat  $q_L$  fluxes are computed with the following expressions proposed by Garratt (1992):

$$q_S = c_a \cdot \rho_a \cdot p_a / p_{0,a} \cdot \frac{\kappa^2 \cdot v_a \cdot (T_a - T_{ice})}{(\ln \frac{h_{AWS}}{z_{ice}})^2} \quad (11)$$

$$q_L = 0.623 \cdot L_s \cdot \rho_a / p_{0,a} \cdot \frac{\kappa^2 \cdot v_a (p_{v,a} - p_{v,ice})}{(\ln \frac{h_{AWS}}{z_{ice}})^2} \quad (12)$$

where  $h_{AWS}$  is the measurement height above the ground surface of the AWS (in  $m$ ),  $v_a$  is the wind speed in  $[m s^{-1}]$  and  $M_F$  denotes fountain water spray mass in  $[kg]$ .  $c_a$  is the specific heat of air at

constant pressure ( $1010 \text{ J kg}^{-1} \text{ K}^{-1}$ ),  $\rho_a$  is the air density at standard sea level ( $1.29 \text{ kg m}^{-3}$ ),  $p_{0,a}$  is the air pressure at standard sea level ( $1013 \text{ hPa}$ ),  $\kappa$  is the von Karman constant (0.4),  $L_s$  is the heat of sublimation ( $2848 \text{ kJ kg}^{-1}$ ) and  $z_{ice}$  ( $1.7 \text{ mm}$ ) denotes the roughness length of ice (momentum and scalar). The vapor pressures over air ( $p_{v,a}$ ) and ice ( $p_{v,ice}$ ) was obtained using the following formulation given in WMO (2018):

$$\begin{aligned} p_{v,a} &= 6.107 \cdot 10^{(7.5 \cdot T_a / (T_a + 237.3))} \\ p_{v,ice} &= (1.0016 + 3.15 \cdot 10^{-6} \cdot p_a - 0.074 \cdot p_a^{-1}) \cdot (6.112 \cdot e^{(22.46 \cdot T_{ice} / (T_{ice} + 272.62))}) \end{aligned} \quad (13)$$

where  $p_a$  is the measured air pressure in  $[hPa]$ .

#### 1.2.4 Fountain water heat flux $q_F$

The total energy flux is further influenced through the heat flux caused by the water that was additionally added to the surface of the Icestupa during the time the fountain was running. We take this interaction between the fountain water and the ice surface into account by assuming that the ice surface temperature remains constant at  $0^\circ \text{C}$  during time steps when the fountain is active. This process can be divided into two simultaneous steps: (a) the water temperature  $T_{water}$  is cooled to  $0^\circ \text{C}$  and (b) the ice surface temperature is warmed to  $0^\circ \text{C}$ . Process (a) transfers the necessary energy for process (b) throughout the fountain runtime. We further assume that this process is instantaneous, i.e. the ice temperature is immediately set to  $0^\circ \text{C}$  within just one time step  $\Delta t$  when the fountain is switched on. Thus, the heat flux caused by the fountain water is calculated as follows:

$$q_F = \begin{cases} 0 & \text{if } \Delta M_F = 0 \\ \frac{\Delta M_F \cdot c_{water} \cdot T_{water}}{\Delta t \cdot A} + \frac{\rho_{ice} \cdot \Delta x \cdot c_{ice} \cdot T_{ice}}{\Delta t} & \text{if } \Delta M_F > 0 \end{cases} \quad (14)$$

with  $c_{ice}$  as the specific heat of ice.

#### 1.2.5 Bulk Icestupa heat flux $q_G$

The bulk Icestupa heat flux  $q_G$  corresponds to the ground heat flux in normal soils and is caused by the temperature gradient between the surface layer ( $T_{ice}$ ) and the ice body ( $T_{bulk}$ ). It is expressed by using the heat conduction equation as follows:

$$q_G = k_{ice} \cdot (T_{bulk} - T_{ice}) / l_{ice} \quad (15)$$

where  $k_{ice}$  is the thermal conductivity of ice ( $2.123 \text{ W m}^{-1} \text{ K}^{-1}$ ),  $T_{bulk}$  is the mean temperature of the ice body within the Icestupa and  $l_{ice}$  is the average distance of any point in the surface to any other point in the ice body.  $T_{bulk}$  is initialised as  $0^\circ \text{C}$  and later determined from Eqn. 15 as follows:

$$T_{bulk}^{i+1} = T_{bulk} - (q_G \cdot A \cdot \Delta t) / (M_{ice} \cdot c_{ice}) \quad (16)$$

Since we assume a conical shape with  $r_{ice} > h_{ice}$ ,  $l_{ice}$  cannot be greater than  $2r_{ice}$  and also cannot be less than  $\Delta x$ . Therefore, the average distance from any point on the surface to any point inside is  $\Delta x \leq l_{ice} \leq r_{ice}$ . We calculate  $q_G$  here assuming  $l_{ice} = r_{ice}/2$ .

### 1.3 Surface Temperature

The available energy  $q_{surf}$  can act on the surface of the AIR to a) change its temperature, b) melt ice or c) freeze ice. So Eqn. 6 can be rewritten as:

$$q_{surf} = q_{freeze/melt} + q_T \quad (17)$$

where  $q_T$ ,  $q_{freeze}$  and  $q_{melt}$  represent energy associated with process (a), (b) and (c) respectively.

To distribute the surface energy flux into these three components, we categorize the model time steps as freezing or melting events.

Freezing events ( $q_{melt} = 0$ ) can only occur if there is fountain water available and the surface energy flux is negative. But just these two conditions are not sufficient as the latent heat energy can only contribute to temperature fluctuations. Therefore, freezing events occur when  $\Delta M_F > 0$  and  $q_{surf} < 0$  and  $(q_{surf} - q_L) < 0$ . Melting events ( $q_{freeze} = 0$ ) occur in the rest of the time steps.

During a freezing event, the available energy ( $q_{surf} - q_L$ ) can either be sufficient or insufficient to freeze the fountain water available. If insufficient, the freezing energy becomes  $q_{freeze} = -\Delta M_F \cdot A \cdot \Delta t / L_f$  and the additional energy further cools down the surface temperature.

$$(q_{freeze}, q_T) = \begin{cases} (q_{surf} - q_L, q_L) & \text{if } (q_{surf} - q_L) < -\Delta M_F \cdot A \cdot \Delta t / L_f \\ (-\frac{\Delta M_F \cdot A \cdot \Delta t}{L_f}, q_{surf} + \frac{\Delta M_F \cdot A \cdot \Delta t}{L_f}) & \text{if } (q_{surf} - q_L) > -\Delta M_F \cdot A \cdot \Delta t / L_f \end{cases} \quad (18)$$

During a melting event, the surface energy flux ( $q_{surf}$ ) is first used to change the temperature to  $T_{temp}$  calculated as:

$$T_{temp} = \frac{q_{surf} \cdot \Delta t}{\rho_{ice} \cdot c_{ice} \cdot \Delta x} + T_{ice}^i \quad (19)$$

If  $T_{temp}^{i+1} > 0^\circ C$ , then energy is reallocated from  $q_T$  to  $q_{melt}$  to reset  $T_{ice}^{i+1} = 0^\circ C$  and produce meltwater.

These steps can be summarised as:

$$(q_{melt}, q_T) = \begin{cases} (0, q_{surf}) & \text{if } T_{temp} < 0 \\ (\frac{T_{temp} \cdot \rho_{ice} \cdot c_{ice} \cdot \Delta x}{\Delta t}, q_{surf} - \frac{T_{temp} \cdot \rho_{ice} \cdot c_{ice} \cdot \Delta x}{\Delta t}) & \text{if } T_{temp} > 0 \end{cases} \quad (20)$$

**Table 1.** Free parameters in the model categorised as constant, uncertain and site parameters. Base value (B) and uncertainty (U) were taken from the literature. For assumptions (assum.), the uncertainty was chosen to be relatively large (5 %). For measurements (meas.), the uncertainty due to parallax errors is chosen to be (1 %).

Constant Parameters	Symbol	Value	References
Van Karman constant	$\kappa$	0.4	B: Cuffey and Paterson
Stefan Boltzmann constant	$\sigma$	$5.67 \cdot 10^{-8} W m^{-2} K^{-4}$	B: Cuffey and Paterson
Air pressure at sea level	$p_{0,a}$	1013 hPa	B: Mölg and Hardy
Density of water	$\rho_w$	$1000 kg m^{-3}$	B: Cuffey and Paterson
Density of ice	$\rho_{ice}$	$917 kg m^{-3}$	B: Cuffey and Paterson
Density of air	$\rho_a$	$1.29 kg m^{-3}$	B: Mölg and Hardy
Specific heat of ice	$c_{ice}$	$2097 J kg^{-1} ^\circ C^{-1}$	B: Cuffey and Paterson
Specific heat of water	$c_w$	$4186 J kg^{-1} ^\circ C^{-1}$	B: Cuffey and Paterson
Specific heat of air	$c_a$	$1010 J kg^{-1} ^\circ C^{-1}$	B: Mölg and Hardy
Thermal conductivity of ice	$k_{ice}$	$2.123 W m^{-1} K^{-1}$	B: Bonales et al.
Latent Heat of Sublimation	$L_s$	$2848 kJ kg^{-1}$	B: Cuffey and Paterson
Latent Heat of Fusion	$L_f$	$334 kJ kg^{-1}$	B: Cuffey and Paterson
Uncertain Parameters		Range	
Precipitation	$T_{ppt}$	$1 ^\circ C$	$\pm 1 ^\circ C$
Temperature threshold			
Ice Emissivity	$\epsilon_{ice}$	0.95	[0.949,0.993]
Ice Albedo	$\alpha_{ice}$	0.35	$\pm 5 \%$
Snow Albedo	$\alpha_{snow}$	0.85	$\pm 5 \%$
Albedo Decay Rate	$\tau$	10 days	[1, 22] days
Surface layer thickness	$\Delta x$	20 mm	[1, 10] mm

## 1.4 Mass Balance

The mass balance equation is used to derive the water that drains away ( $M_{runoff}$ ) as follows:

$$\frac{\Delta M_{runoff}}{\Delta t} = \frac{\Delta M_F + \Delta M_{ppt} + \Delta M_{dpt} + \Delta M_{cdt} - \Delta M_{ice} - \Delta M_{melt} - \Delta M_{vapour}}{\Delta t} \quad (21)$$

where  $\Delta M = M^i - M^{i-1}$ . Here  $\frac{\Delta M_F}{\Delta t} = d_F$  where  $d_F$  is the spray of the fountain measured in [ $kg s^{-1}$ ];  $M_{ppt}$  is the cumulative precipitation;  $M_{dpt}$  is the cumulative accumulation through water vapour deposition;  $M_{cdt}$  is the cumulative accumulation through water vapour condensation;  $M_{ice}$  is the cumulative mass of ice;  $M_{melt}$  is the cumulative mass of melt water and  $M_{vapour}$  represents the cumulative water vapor loss by evaporation or sublimation.

Precipitation input is calculated as:

$$\frac{\Delta M_{ppt}}{\Delta t} = \begin{cases} \pi \cdot r_{ice}^2 \cdot \rho_w \cdot ppt & \text{if } T_a < T_{ppt} \\ 0 & \text{if } T_a \geq T_{ppt} \end{cases} \quad (22)$$

where  $\rho_w$  is the density of water ( $1000 \text{ kg m}^{-3}$ ),  $ppt$  is the measured precipitation rate in  $[\text{m s}^{-1}]$  and  $T_{ppt}$  is the temperature threshold below which precipitation falls as snow. Here, snowfall events were identified using  $T_{ppt}$  as  $1^\circ\text{C}$ . Snow mass input is calculated by assuming a uniform deposition over the entire circular footprint of the Icestupa.

The latent heat flux is used to estimate either the evaporation and condensation processes or sublimation and deposition processes. During time steps at which surface temperature is below  $0^\circ\text{C}$  only sublimation and deposition can occur, but if the surface temperature reaches  $0^\circ\text{C}$ , evaporation and condensation can also occur. As the differentiation between evaporation and sublimation (and condensation and deposition) when the air temperature reaches  $0^\circ\text{C}$  is difficult, we assume that negative (positive) latent heat fluxes correspond only to sublimation (deposition), i.e. no evaporation (condensation) is calculated.

$$\left(\frac{\Delta M_{vapour}}{\Delta t}, \frac{\Delta M_{dpt}}{\Delta t}\right) = \begin{cases} (-q_L \cdot A/L_s, 0) & \text{if } q_L < 0 \\ (0, q_L \cdot A/L_s) & \text{if } q_L \geq 0 \end{cases} \quad (23)$$

Using the melt energy  $q_{melt}$ , we estimate the frozen and melted ice mass ( $\Delta M_{ice}$ ,  $\Delta M_{melt}$ ). Removing the contribution of precipitation and combining Eqn. 23, we are left with the contribution from the melt energy as follows:

$$\left(\frac{\Delta M_{ice} + \Delta M_{vapour} - \Delta M_{dpt} - \Delta M_{ppt}}{\Delta t}, \frac{\Delta M_{melt}}{\Delta t}\right) = \begin{cases} \frac{q_{melt} \cdot A}{L_f} \cdot (-1, 1) & \text{if } q_{melt} \geq 0 \\ \frac{q_{melt} \cdot A}{L_f} \cdot (-1, 0) & \text{if } q_{melt} < 0 \text{ and } \frac{\Delta M_F}{\Delta t} \geq -\frac{q_{melt} \cdot A}{L_f} \\ \left(\frac{\Delta M_F}{\Delta t}, 0\right) & \text{if } q_{melt} < 0 \text{ and } 0 \leq \frac{\Delta M_F}{\Delta t} < -\frac{q_{melt} \cdot A}{L_f} \end{cases} \quad (24)$$

Now, with all the other terms known in Eqn. 21, the water drainage/runoff can be determined.

Considering AIRs as water reservoirs, we can quantify their potential through the amount of water they store (storage quantity) and the length of time they store it (storage duration). Another means of comparing different Icestupas is through their water storage efficiency defined accordingly as:

$$\text{Storage Efficiency} = \frac{M_{melt}}{(M_F + M_{ppt} + M_{dpt} + M_{cdt})} \cdot 100 \quad (25)$$

## REFERENCES

- Bonales, L. J., Rodriguez, A. C., and Sanz, P. D. (2017). Thermal conductivity of ice prepared under different conditions. *International Journal of Food Properties* 20, 610–619. doi:10.1080/10942912.2017.1306551
- Cuffey, K. M. and Paterson, W. S. B. (2010). *The Physics Of Glaciers* (Elsevier)
- Fujita, K. and Ageta, Y. (2000). Effect of summer accumulation on glacier mass balance on the tibetan plateau revealed by mass-balance model. *Journal of Glaciology* 46, 244–252. doi:10.3189/172756500781832945
- Garratt, J. R. (1992). *The Atmospheric Boundary Layer* (Cambridge University Press)
- Hock, R. (2005). Glacier melt: a review of processes and their modelling. *Progress in Physical Geography: Earth and Environment* 29, 362–391



- 152 Hori, M., Aoki, T., Tanikawa, T., Motoyoshi, H., Hachikubo, A., Sugiura, K., et al. (2006). In-situ  
153 measured spectral directional emissivity of snow and ice in the 8–14 micrometer atmospheric window.  
154 *Remote Sensing of Environment* 100, 486 – 502
- 155 Mölg, T. and Hardy, D. R. (2004). Ablation and associated energy balance of a horizontal glacier surface  
156 on kilimanjaro. *J. Geophys. Res.-Atmos.* 109, 1–13. doi:10.1029/2003JD004338
- 157 Oerlemans, J. and Knap, W. H. (1998). A 1 year record of global radiation and albedo in the  
158 ablation zone of morteratschgletscher, switzerland. *Journal of Glaciology* 44, 231–238. doi:10.  
159 3189/S0022143000002574
- 160 Schmidt, L. S., Aðalgeirsdóttir, G., Guðmundsson, S., Langen, P. L., Pálsson, F., Mottram, R., et al. (2017).  
161 The importance of accurate glacier albedo for estimates of surface mass balance on vatnajökull: evaluating  
162 the surface energy budget in a regional climate model with automatic weather station observations. *The*  
163 *Cryosphere* 11, 1665–1684. doi:10.5194/tc-11-1665-2017
- 164 WMO (2018). *Guide to Instruments and Methods of Observation* (World Meteorological Organization ;  
165 2018 (2018 Edition))
- 166 Woolf, H. M. (1968). *On the Computation of Solar Elevation Angles and the determination of sunrise and*  
167 *sunset times* (National Aeronautics and Space Administration)
- 168 Zhou, S., Kang, S., Gao, T., and Zhang, G. (2010). Response of zhadang glacier runoff in nam co basin,  
169 tibet, to changes in air temperature and precipitation form. *Chinese Science Bulletin* 55, 2103–2110.  
170 doi:10.1007/s11434-010-3290-5